

1 **The Importance of Adsorption for CCN Activity and** 2 **Hygroscopic Properties of Mineral Dust Aerosol**

3

4 **Prashant Kumar¹, Athanasios Nenes^{1,2}, and Irina N. Sokolik²**

5 ¹School of Chemical & Biomolecular Engineering, Georgia Institute of Technology,
6 Atlanta, GA, 30332, USA

7 ²School of Earth & Atmospheric Sciences, Georgia Institute of Technology, Atlanta, GA,
8 30332, USA

9 Correspondence to: A. Nenes (athanasios.nenes@gatech.edu)

10 **Abstract**

11 This study uses published data on dust-water interactions to examine the importance
12 of including water adsorption effects when describing the hygroscopic and cloud
13 condensation nuclei (CCN) behavior of mineral dust aerosol. Adsorption activation
14 theory (AT) better represents fresh dust-water interactions than Köhler theory (KT), as *i*)
15 a consistent set of adsorption parameters can describe the hygroscopic behavior of dust
16 (under both sub and supersaturated conditions), *ii*) the dependence of critical
17 supersaturation, s_c , with particle dry diameter, D_{dry} , is closer to observations. The long
18 adsorption timescale could also contribute to the large differences observed between dry
19 and wet generated dust hygroscopicity. If KT and AT are consistently applied to the same
20 dust size distribution, KT predicts up to tenfold higher CCN and 40% higher droplet
21 number concentration than AT. This profoundly different behavior between the theories
22 suggests that both may be required for a comprehensive description of atmospheric dust
23 CCN activity.

24 **1. Introduction**

25 Mineral dust is ubiquitous in the atmosphere and represents a dominant type of
26 particulate matter by mass. Dust particles can act as cloud condensation nuclei (CCN),
27 giant CCN (GCCN) (e.g., Rosenfeld et al., 2001; Levin and Cotton, 2008), or ice nuclei
28 (IN) (e.g., DeMott et al., 2003; Field et al., 2006) affecting cloud microphysics, albedo,
29 and lifetime. Despite its well-recognized importance, assessments of dust impacts on
30 clouds and climate are highly uncertain. In this study, we address the role of dust as CCN
31 with the goal to provide an improved representation of dust CCN activation in the climate
32 models.

33 Dust CCN activity is currently described by Köhler theory (herein KT; Köhler,
34 1936), which is based solely on the contribution of the solute and curvature effects upon
35 water equilibrium vapor pressure. KT implies that dust particles devoid of any solute
36 would require very high ambient supersaturations (dictated by the Kelvin equation) to act
37 as CCN. It is well known however that adsorption of water on insoluble particles
38 (especially clays) can lead to hygroscopic growth similar to deliquescent salts (e.g.,
39 Schuttlefield et al., 2007). Past studies have demonstrated that calcite (CaCO_3) (a mineral
40 with very low solubility compared to deliquescent salts) and Arizona Test Dust (ATD)
41 can interact with water vapor and adsorb multiple layers of water under subsaturated
42 conditions (Gustafsson et al., 2005; Vlasenko et al., 2005; Hatch et al., 2008). This
43 interaction implies that dust mixtures and individual minerals with hydrophilic insoluble
44 surfaces can affect water activity of aerosol (especially when the solute fraction of
45 particles is low) with largely ignored implications for predicted CCN activity. Henson
46 (2007) and Sorjamaa and Laaksonen (2007) recognized this gap, and developed

47 adsorption activation theory (AT) to describe the activation of hydrophilic insoluble
48 CCN. The Sorjamaa and Laaksonen (2007) formulation is based on the FHH (Frenkel,
49 Halsey and Hill) adsorption model (and constrained by two adjustable parameters, A_{FHH} ,
50 B_{FHH}). Kumar et al. (2009) incorporated FHH-AT into a droplet activation
51 parameterization for use in regional and global models, assuming that the aerosol
52 constitutes an external mixture of “soluble” (KT) and “insoluble” (AT) particles.

53 Even if constrained by the same CCN activity or hygroscopic growth data, predicted
54 CCN concentration and cloud droplet number, N_d , can differ between using KT and
55 FHH-AT because: *i*) the relationship between particle critical supersaturation, s_c , and dry
56 diameter, D_{dry} , differs between theories, resulting in a different predicted CCN spectrum
57 even if the same size distribution is used, and, *ii*) KT particles require substantially more
58 water to activate than FHH-AT particles with the same s_c (Kumar et al., 2009).
59 Competition for water vapor in a cloud parcel during activation of KT particles can thus
60 be more intense than for FHH-AT particles, leading to a different parcel maximum
61 supersaturation, s_{max} , and droplet number.

62 In this study, we substantiate the importance of considering water vapor adsorption
63 effects on the activation of mineral dust particles. This is done by fitting published CCN
64 activity and hygroscopic growth data to the KT and FHH-AT, and examining whether
65 each theory can *i*) describe subsaturated hygroscopic growth and CCN activity with one
66 set of water-interaction parameters, and, *ii*) reproduce the observed dependence of s_c with
67 respect to D_{dry} . Finally, we evaluate the differences in the CCN number and droplet
68 number concentrations predicted by KT and FHH-AT, using the consistent parameters
69 and the same aerosol size distribution.

70 **2. Comparison of Köhler and Adsorption Activation Theories**

71 KT provides a relationship between the equilibrium vapor pressure of an aqueous
72 droplet as a function of its wet diameter and exhibits a maximum value termed as critical
73 supersaturation, s_c , at a characteristic critical wet diameter, D_c . Particles exposed to
74 ambient supersaturation above s_c typically activate into cloud droplets (Nenes et al.,
75 2001). In KT, s_c depends on the amount of solute in the dry particle, which is related to
76 its chemical composition and size. Petters and Kreidenweis (2007) parameterized the
77 solute term of KT in terms of a hygroscopicity parameter, κ , which was derived from the
78 relationship between D_{dry} and s_c . κ can be used to directly compare the hygroscopicity of
79 aerosol over a wide range of composition, with $\kappa \rightarrow 0$ for completely insoluble particles
80 (for which $s_c \sim D_{dry}^{-1}$) to $\kappa \rightarrow 1.4$ for the most hygroscopic atmospheric aerosol (for which
81 $s_c \sim D_{dry}^{-3/2}$). According to KT, a constant value of κ should be able to describe both
82 aerosol subsaturated water uptake (where relative humidity, RH, is below 100%) and
83 predict CCN activity (RH > 100%).

84 FHH-AT is similar to KT, except that the solute term is replaced with an adsorption
85 term modeled by the FHH isotherm (Crittenden and Thomas, 1998). The adsorption
86 parameter B_{FHH} , strongly affects the shape of the equilibrium curve, and largely
87 determines the existence and value of s_c and D_c (Kumar et al., 2009). As with KT, s_c in
88 FHH-AT can be related to D_{dry} as $s_c = CD_{dry}^x$. Particles with an appreciable soluble
89 fraction follow KT, and $x \sim -1.5$ when $\kappa > 0.2$. In FHH-AT, x varies between -0.8 and -1.5,
90 depending on A_{FHH} , B_{FHH} (Kumar et al., 2009).

91

92 3. Evidence for Adsorption Activation

93 Figure 1a shows published data (symbols) of s_c as a function of D_{dry} (Koehler et al.
94 2009; Sullivan et al., 2009) for different dust types and individual mineral particles
95 generated in the lab either with the use of a dry fluidized bed, or via wet atomization from
96 an aqueous suspension of dust particles. The CCN activity data are fitted to a power law
97 expression, $s_c = CD_{dry}^x$, from which the “experimental” exponent, x_{exp} , is determined
98 (Table 1). A_{FHH} and B_{FHH} and the corresponding exponent, x_{FHH} , were determined from
99 fitting the FHH-AT model (Figure 1a, lines) to the experimental data via least squares
100 minimization. The KT fits to the data (expressed in terms of κ) are given by Koehler et al.
101 (2009) and Sullivan et al. (2009), from which the corresponding KT exponent, x_κ , is
102 computed. The values of the exponents, adsorption parameters (A_{FHH} , B_{FHH}), and κ
103 (determined by Koehler et al., 2009, and Sullivan et al., 2009) are presented in Table 1.

104 In Figure 1b, x_κ (circles) and x_{FHH} (squares) are plotted against x_{exp} for all dust
105 samples and individual minerals. With the exception of CaCO_3 and CaSO_4 (calcium
106 sulphate) (where $x_\kappa \rightarrow -1$ because of the very low κ), $x_\kappa \sim -1.5$. CaCO_3 (representing fresh
107 unprocessed dust) and CaSO_4 , $\text{CaC}_2\text{O}_4 \cdot \text{H}_2\text{O}$ (calcium oxalate monohydrate or COH)
108 (representing atmospherically processed mineral dust) are better described by FHH-AT,
109 as x_{FHH} is in perfect agreement with x_{exp} . For wet-generated ATD, Owens Lake (OL),
110 Canary Island Dust (CID), and oxalic acid ($\text{C}_2\text{O}_4\text{H}_2$), x_{FHH} lies closer than x_κ to the 1:1
111 line. x_κ for dry Saharan Dust (SD), ATD and wet $\text{Ca}(\text{NO}_3)_2$ are closer to x_{exp} than x_{FHH} ;
112 this is expected for $\text{Ca}(\text{NO}_3)_2$ because it is highly soluble (deliquescence $\text{RH} = 49\%$;
113 Fountoukis and Nenes, 2007), but not for dry ATD and SD. The large scatter ($\text{R}^2 < 0.7$

114 for the s_c - D_{dry} data for dry ATD) and potential size-dependant composition (for SD) may
 115 explain this.

116 Another indication that KT may be an incomplete description of the dust CCN
 117 activity presents itself in the value of wet-dust κ parameters, and the implications thereof.
 118 If the aerosol can be considered as a mixture of a soluble salt with molar volume
 119 (M_s/ρ_s) , effective van't Hoff factor ν_s , and volume fraction ε_s , then

120
$$\kappa = \left(\frac{M_w}{\rho_w} \right) \left(\frac{\rho_s \nu_s}{M_s} \right) \varepsilon_s$$
, where (M_w/ρ_w) is the molar volume of water. Assuming that the

121 hygroscopic fraction of dust behaves like ammonium sulfate gives $\left(\frac{M_w}{\rho_w} \right) \left(\frac{\rho_s \nu_s}{M_s} \right) = 0.61$

122 (Petters and Kreidenweis, 2007). Therefore, the dust κ parameters can be used to infer an
 123 “equivalent soluble volume fraction”, computed as $\varepsilon_s = \frac{\kappa}{0.61}$. If KT indeed applies, then

124 ε_s should reflect the true soluble fraction of dust. From the values of κ reported in Table
 125 1, $\varepsilon_s = 0.58, 0.65$ - 1.78 , and 0.43 for wet ATD, OL, and CID, respectively. Such a large
 126 soluble fraction in fresh dust is much larger (or even impossible if larger than unity) than
 127 the expected 2% soluble mass fraction in ATD (Vlasenko et al., 2005) and 3-37% in OL
 128 (Koehler, 2008). Koehler et al. (2009) attribute this enhanced hygroscopicity to
 129 redistribution of the soluble material among the insoluble dust cores, particularly in the
 130 smaller size range. Given that KT implies $s_c \sim \varepsilon_s^{-0.5} D_{dry}^{-1.5}$, ε_s will have to scale with $D_{dry}^{0.3}$
 131 for KT to yield $x_\kappa = x_{exp} \sim -1.36$. This means that ε_s varies more than 60% over the
 132 diameter range (40 – 200nm) reported in the Koehler et al. (2009) experiments, so that
 133 the soluble fraction at the high s_c should be close to unity. This is certainly possible; the

134 hygroscopicity parameter, however, does not seem to change considerably when subsets
135 of the activation data (especially in the higher supersaturation range) are separately
136 considered. This implies that KT may not completely describe the CCN activity of dust,
137 so that other processes, such as physisorption, could contribute to the water activity
138 depression required to yield the observed CCN activity. The long equilibration time
139 (minutes or more) associated with adsorption (e.g., Schuttlefield et al., 2007) may explain
140 why the hygroscopicity of dry and wet generated dust are so different. The residence time
141 of dust particles in the instrumentation is typically less than a minute, limiting the amount
142 of water that can adsorb and bias the observed hygroscopicity below its equilibrium
143 value. Wetting the dust particles prior to measurement would maximize the amount of
144 adsorbed water and express the full extent of its hygroscopicity. One approach to
145 modeling this system is using one value for A_{FHH} , B_{FHH} , combined with a variable uptake
146 coefficient (that is very low during formation of the monolayer, and progressively
147 increases with the number of adsorbed layers). Another explanation is the swelling of
148 clays; during complete wetting, more surface area could be exposed for interaction,
149 which would enhance dust hygroscopicity compared to a dry particle. Future work should
150 focus on the existence and mechanism of adsorption/desorption transients.

151 **4. Reconciling Dust Hygroscopicity under Subsaturated and Supersaturated** 152 **Conditions.**

153 Herich et al. (2009) measured water uptake on mineral dusts and different clays
154 under subsaturated (with a hygroscopicity tandem differential mobility analyzer;
155 HTDMA) and supersaturated (with a cloud condensation nuclei counter; CCNc)
156 conditions. The hygroscopic growth factors (GF) were measured with a HTDMA, and the

157 CCN activity was measured using a CCNc. A poor correlation in experiments (deviation
158 larger than $\pm 50\%$) was found between κ derived from the HTDMA and CCNc. Herich et
159 al. (2009) attributed this to resolution limitations in the HTDMA GF. Alternatively, KT
160 may not adequately represent dust-water interactions, so that a single value of κ is not
161 expected to describe the subsaturated water uptake and CCN activity for mineral dust
162 aerosol. If FHH is more appropriate, then one set of A_{FHH} and B_{FHH} (neglecting the
163 potential non-equilibrium artifacts) should reproduce both subsaturated and
164 supersaturated properties of mineral dust aerosol, and is attempted below.

165 Gustafsson et al. (2005) studied the subsaturated hygroscopic uptake of ATD
166 particles generated from suspensions in distilled water. Surface coverages as a function of
167 RH were measured using a thermogravimetric analysis, during which multilayer
168 adsorption (the number of water molecule layers, $\theta \sim 3 - 4$) were observed for RH greater
169 than 50%. Under such conditions, the FHH adsorption isotherm is applicable and is fitted
170 to the data. The optimal values for A_{FHH} and B_{FHH} are 1.16 and 0.88, respectively, versus
171 0.85 and 0.88 from CCN activation experiments (Table 1). Vlasenko et al. (2005)
172 measured subsaturated hygroscopic growth of dry ATD; fitting a FHH adsorption
173 isotherm to the growth data for $RH > 70\%$ gives $A_{FHH} = 0.19$ and $B_{FHH} = 0.98$ (RMSE =
174 0.035), which are very close to the FHH parameters obtained from CCN activation
175 experiments for the same compound ($A_{FHH} = 0.27$ and $B_{FHH} = 0.79$; Table 1). Fitting FHH
176 isotherms to the Gustafsson et al. (2005) and Hatch et al. (2008) measurements for
177 CaCO_3 (different type from Table 1) gives $A_{FHH} = 0.83-1.00$ and $B_{FHH} = 0.76$. All the
178 above suggests that the adsorption parameters for similar samples are indeed consistent
179 across different studies.

180 **5. Impact of KT and AT on CCN and Droplet Number**

181 In this section, differences in predicted CCN concentrations and droplet number
182 concentrations from application of KT and FHH-AT are estimated. For this, we use a
183 single-mode lognormal aerosol obtained from in-situ measurements of SD during the
184 NAMMA field campaign (Twohy et al., 2009) (with geometric mean diameter, $D_g = 0.10$
185 μm , standard deviation, $\sigma_g = 1.6$, and total particle concentration, $N_0 = 225$ per cm^3). The
186 CCN spectra computed with KT and FHH-AT (using κ , A_{FHH} , and B_{FHH} listed in Table 1
187 and the lognormal CCN spectra formulations of Kumar et al., 2009) are presented in
188 Figure 2a. For supersaturations between 0.05% and 0.5% (a range relevant for cumulus
189 and stratocumulus clouds), application of KT results in 8-12 times larger CCN than when
190 applying FHH-AT. This is a direct consequence of $x_\kappa < x_{FHH}$, which tends to yield a larger
191 activation fraction for KT-derived CCN spectra. For supersaturations greater than 0.5%,
192 most aerosol in both distributions activate, so CCN computed by KT and FHH-AT
193 converge.

194 The larger CCN concentrations (at a given supersaturation) associated with use of
195 KT suggests that the calculated droplet number, compared to using FHH-AT, will be
196 larger. KT however requires more water to activate particles than FHH-AT (Kumar et al.,
197 2009), so the competition for water vapor in the former particles is stronger, potentially
198 impacting s_{max} and N_d . For example for $s_c = 0.05\%$, the ratio of water volume at D_c in KT
199 against FHH-AT ranges from 4.83 (dry ATD) to 15.43 (wet ATD). Hence for the same
200 size distribution, the droplet number difference from application of each theory depends
201 on two competing factors: *i*) the stronger competition of KT CCN for water vapor, and *ii*)
202 the typically larger activation fraction associated with KT. These factors are

203 comprehensively accounted for in droplet number calculations carried out with the
 204 Kumar et al. (2009) parameterization. In all droplet number calculations presented, the
 205 parcel is assumed adiabatic, with initial temperature, 273 K; pressure, 600 mbar; and
 206 updraft velocity, w ranging from 0.1 ms^{-1} to 10 ms^{-1} . For each dust type, the respective κ
 207 and FHH parameters (A_{FHH} and B_{FHH}) from Table 1 are used.

208 Figure 2b shows the ratio of total CCN that activate to cloud droplets using KT, N_d^κ ,
 209 to that from FHH-AT, N_d^{FHH} , as a function of parcel updraft velocity (symbols) for four
 210 different dust types. The corresponding parcel s_{max} is also shown (solid lines). For wet
 211 CID and wet ATD, $\frac{N_d^\kappa}{N_d^{FHH}}$ is largest ($\sim 1.3 - 1.4$) at $w \sim 0.1 \text{ ms}^{-1}$ and approaches 1.0 for w
 212 $> 1 \text{ ms}^{-1}$. This is because the parcel $s_{max} < 1\%$ for all $w < 1 \text{ ms}^{-1}$ (Figure 2b), where
 213 $\frac{F_k}{F_{FHH}} > 1$ (Figure 2a) and droplet differences are dominated by the larger activation
 214 fractions associated with KT. Similarly, $\frac{F_k}{F_{FHH}} > 1$ for dry ATD and SD and $w < 1 \text{ ms}^{-1}$.
 215 However, for $w > 1 \text{ ms}^{-1}$, the competition of water vapor from KT particles is sufficiently
 216 strong so that $\frac{N_d^\kappa}{N_d^{FHH}} < 1$. At very high updrafts ($> 3 \text{ ms}^{-1}$), all particles activate,
 217 and $\frac{N_d^\kappa}{N_d^{FHH}} \rightarrow 1$.

218 6. Conclusions.

219 In this study, we compared Köhler theory (KT) against FHH adsorption activation
 220 theory (FHH-AT) when applied to the activation of mineral dust aerosol. Based on

221 published data, a number of potential issues were found with KT, suggesting it may not
222 fully represent CCN activity of mineral dust aerosol, since *i*) a consistent set of FHH-AT
223 adsorption parameters can be found that describe both the subsaturated hygroscopic
224 growth and CCN activity, and, *ii*) the critical supersaturation vs dry diameter exponents
225 determined for FHH-AT are often closer to observations, than those from KT.
226 Application of KT and FHH-AT leads to the differences in predicted CCN and cloud
227 droplet number concentrations, even if consistent hygroscopicity and adsorption
228 parameters (i.e., derived from the same experimental data) are used. For the dust samples
229 considered here, CCN concentrations can differ by a factor of 10, and results in a 40%
230 difference in predicted cloud droplet number concentration. Thus, a comprehensive
231 description of CCN activity of mineral dust aerosol throughout its atmospheric lifetime
232 may require a combination of both KT and FHH-AT.

233 **Acknowledgements**

234 This work was supported by the NOAA ACC Program. AN acknowledges support from
235 NSF CAREER and NASA-ACMAP grants.

236 **References**

- 237 Crittenden, B. D., and W. J. Thomas (1998), Adsorption technology and design,
238 Butterworth-Heinemann, ISBN 0750619597.
- 239 DeMott, P. J., K. Sassen, M. R. Poellot, D. Baumgardner, D. C. Rogers, S. D. Brooks, A.
240 J. Prenni, and S. M. Kreidenweis (2003), African dust aerosols as atmospheric ice
241 nuclei, *Geophys. Res. Lett.*, 30(14), 1732, doi:10.1029/2003GL017410.

242 Field, P. R., O. Möhler, P. Connolly, M. Krämer, R. Cotton, A. J. Heymsfield, H.
243 Saathoff, and M. Schnaiter (2006), Some ice nucleation characteristics of Asian and
244 Saharan desert dust, *Atmos. Chem. Phys.*, 6, 2991-3006.

245 Fountoukis, C., and A. Nenes (2007), ISORROPIA II: a computationally efficient aerosol
246 thermodynamic equilibrium model for K^+ , Ca^{2+} , Mg^{2+} , NH_4^+ , Na^+ , SO_4^{2-} , NO_3^- , Cl^- ,
247 H_2O aerosols, *Atmos. Chem. Phys.*, 7, 4639-4659.

248 Gustafsson, R. J., A. Orlov, C. L. Badger, P. T. Griffiths, R. A. Cox, and R. M. Lambert
249 (2005), A comprehensive evaluation of water uptake on atmospherically relevant
250 mineral surfaces: DRIFT spectroscopy, thermogravimetric analysis and aerosol
251 growth measurements, *Atmos. Chem. Phys.*, 5, 3415–3421.

252 Hatch, C. D., K. M. Gierlus, J. D. Schuttlefield, and V. H. Grassian (2008), Water
253 adsorption and cloud condensation nuclei activity of calcite and calcite coated with
254 model humic and fulvic acids, *Atmos. Environ.*, 42, 5672-5684.

255 Herich, H., T. Tritscher., A. Wiacek, M. Gysel, E. Weingartner, U. Lohmann, U.
256 Baltensperger, and D. J. Cziczo (2009), Water uptake of clay and desert dust
257 aerosol particles at sub- and supersaturated water vapor conditions, *Phys. Chem.*
258 *Chem. Phys.*, doi:10.1039/b901585j.

259 Henson, B. F. (2007), An adsorption model of insoluble particle activation: Application
260 to black carbon, *J. Geophys. Res.*, 112, D24S16, doi:10.1029/2007JD008549.

261 Koehler, K. A. (2008), The impact of natural dust aerosol on warm and cold cloud
262 formation, Ph.D. dissertation thesis, 208 pp., Colo. State Univ., Fort Collins.

263 Koehler, K. A., S. M. Kreidenweis, P. J. DeMott, M. D. Petters, A. J. Prenni, and C. M.
264 Carrico (2009), Hygroscopicity and cloud droplet activation of mineral dust aerosol,
265 *Geophys. Res. Lett.*, *36*, L08805, doi:10.1029/2009GL037348.

266 Köhler, H. (1936), The nucleus in and the growth of hygroscopic droplets, *Trans. Faraday*
267 *Soc.*, *32*(2), 1152-1161.

268 Kumar, P., I. N. Sokolik, and A. Nenes (2009), Parameterization of cloud droplet
269 formation for global and regional models: including adsorption activation from
270 insoluble CCN, *Atmos. Chem. Phys.*, *9*, 2517-2532.

271 Levin, Z., and W. R. Cotton (2007), Aerosol pollution impact on precipitation: A
272 scientific review, WMO/IUGG Report.

273 Nenes., A., S. Ghan, H. Abdul-Razzak, P. Y. Chuang, and J. H. Seinfeld (2001), Kinetic
274 Limitations on Cloud Droplet Formation and Impact on Cloud Albedo, *Tellus*, *53B*,
275 133-149.

276 Petters, M. D., and S. M. Kreidenweis (2007), A single parameter representation of
277 hygroscopic growth and cloud condensation nucleus activity, *Atmos. Chem. Phys.*,
278 *7*, 1961-1971.

279 Rosenfeld, D., Y. Rudich, and R. Lahav (2001), Desert dust suppressing precipitation: A
280 possible desertification feedback loop, *Proc. Natl. Acad. Sci. U.S.A.*, *98*(11), 5975-
281 5980.

282 Schuttlefield, J. D., D. Cox, and V. H. Grassian (2007), An investigation of water uptake
283 on clays minerals using ATR-FTIR spectroscopy coupled with quartz crystal
284 microbalance measurements, *J. Geophys. Res.*, *112*, D21303,
285 doi:10.1029/2007JD008973.

286 Sorjamaa, R. and A. Laaksonen (2007), The effect of H₂O adsorption on cloud drop
287 activation of insoluble particles: a theoretical framework, *Atmos. Chem. Phys.*, 7,
288 6175-6180.

289 Sullivan, R. C., M. J. K. Moore, M. D. Petters, S. M. Kreidenweis, G. C. Roberts, and K.
290 A. Prather (2009), Effect of chemical mixing state on the hygroscopicity and cloud
291 nucleation properties of calcium mineral dust particles, *Atmos. Chem. Phys.*, 9,
292 3303-3316.

293 Twohy, C. H., S. M. Kreidenweis, T. Eidhammer, E. V. Browell, A. J. Heymsfield, A.
294 R. Bansemer, B. E. Anderson, G. Chen, S. Ismail, P. J. DeMott, and S. C. Van Den
295 Heever (2009), Saharan dust particles nucleate droplets in eastern Atlantic clouds,
296 *Geophys. Res. Lett.*, 36, L01807, doi:10.1029/2008GL035846.

297 Vlasenko, A., S. Sjögren, E. Weingartner, H. W. Gäggeler, and M. Ammann (2005),
298 Generation of Submicron Arizona Test Dust Aerosol: Chemical and Hygroscopic
299 Properties, *Aer. Sci. Tech.*, 39 (5), 452-460.

300 **Table 1:** FHH parameters for different mineral dusts and dust related compounds
 301 composites. FHH adsorption activation fits to the experimental CCN activity data
 302 obtained from Koehler et al. (2009) and Sullivan et al. (2009).

| Description (Acronym) | Generation* | κ | A_{FHH} | B_{FHH} | x_{κ} | x_{FHH} | x_{exp} |
|---|-------------|-----------|-----------|-----------|--------------|-----------|-----------|
| Arizona Test Dust (ATD) | Dry | 0.025 | 0.27 | 0.79 | -1.43 | -1.20 | -1.39 |
| Arizona Test Dust (ATD) | Wet | 0.35 | 0.85 | 0.88 | -1.49 | -1.26 | -1.36 |
| Owens Lake (OL) | Wet | 0.39-1.07 | 1.14 | 0.91 | -1.50 | -1.25 | -1.36 |
| Canary Island Dust (CID) | Wet | 0.26 | 0.80 | 0.88 | -1.49 | -1.24 | -1.33 |
| Saharan Dust (SD) | Dry | 0.054 | 0.42 | 0.83 | -1.47 | -1.23 | -1.42 |
| Calcium Nitrate (Ca(NO ₃) ₂) | Wet | 0.51 | 1.13 | 0.90 | -1.50 | -1.30 | -1.59 |
| Oxalic Acid (C ₂ O ₄ H ₂) | Wet | 0.50 | 1.02 | 0.90 | -1.50 | -1.27 | -1.35 |
| Calcium Carbonate (CaCO ₃) | Dry | 0.0011 | 0.25 | 1.19 | -1.18 | -0.96 | -0.96 |
| Calcium Sulfate (CaSO ₄) | Dry | 0.0016 | 0.10 | 0.91 | -1.21 | -1.02 | -1.02 |
| Calcium Oxalate Monohydrate (COH or CaC ₂ O ₄ .H ₂ O) | Dry | 0.048 | 0.57 | 0.88 | -1.47 | -1.15 | -1.16 |

303 *"Dry" refers to dust particles generated with a fluidized bed; "Wet" refers to atomization from an
 304 aqueous solution/suspension

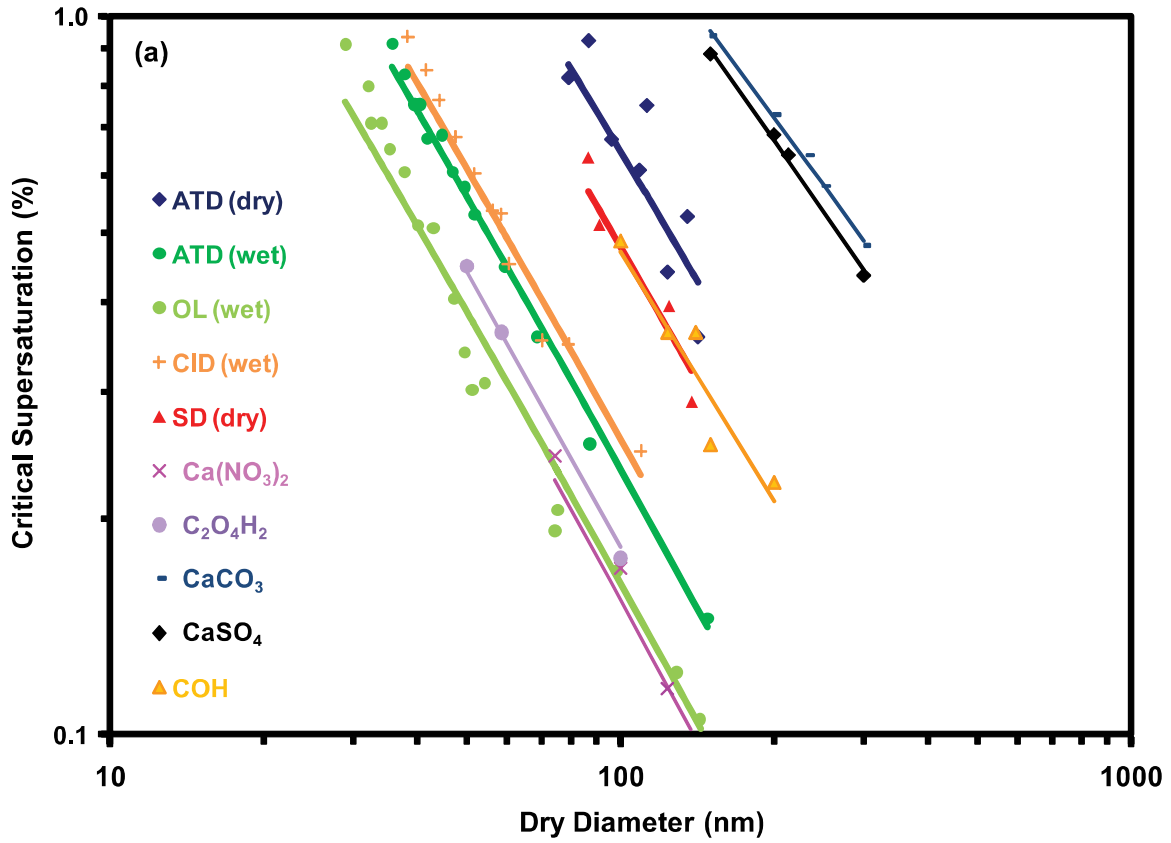
305 **Figure Captions**

306 **Figure 1. (a):** FHH adsorption activation fits (lines) to the observed CCN activity
307 (points) for dust types presented in Table 1. Data obtained from Figure 7.1 (pp 154) and
308 Figure 5 from Koehler et al. (2009) and Sullivan et al. (2009), respectively. “Dry” refers
309 to dust particles generated with a fluidized bed, and “wet” refers to atomization from an
310 aqueous suspension. **(b):** Comparison between x_{exp} , x_{κ} (circles) and x_{FHH} (squares). Color
311 scheme identical to (a). Dashed lines represent $\pm 7.5\%$ deviation from 1:1 line.

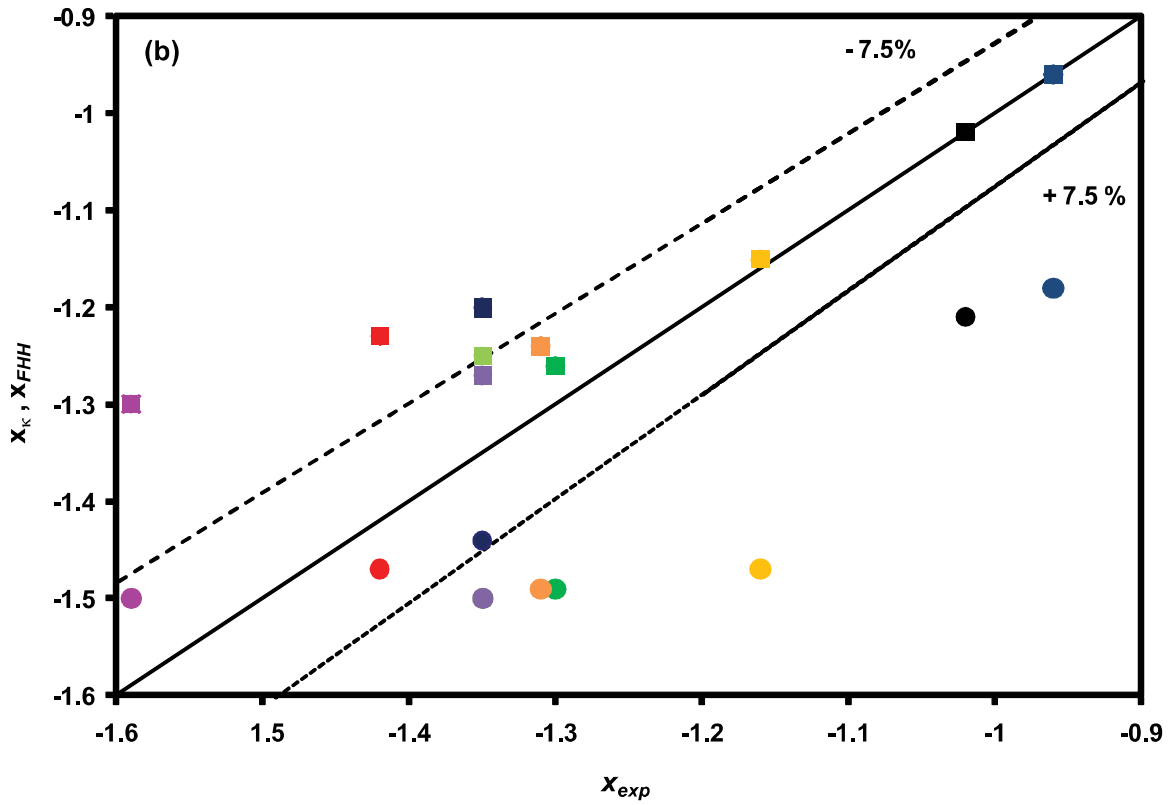
312

313 **Figure 2: (a):** Ratio of CCN spectrum given by Köhler theory to that given by FHH
314 adsorption activation theory as a function of supersaturation. Numbers noted on each
315 curve refer to the ratio of water volume required by KT over FHH-AT to activate a CCN
316 with $s_c = 0.05\%$. **(b):** Ratio of parameterized activated fraction (points) for different dust
317 types as a function of increasing updraft velocity in a cloud parcel. Also shown are the
318 corresponding parcel s_{max} (lines) for each dust type. Color scheme identical to (a). Dust
319 types defined in Table 1.

320

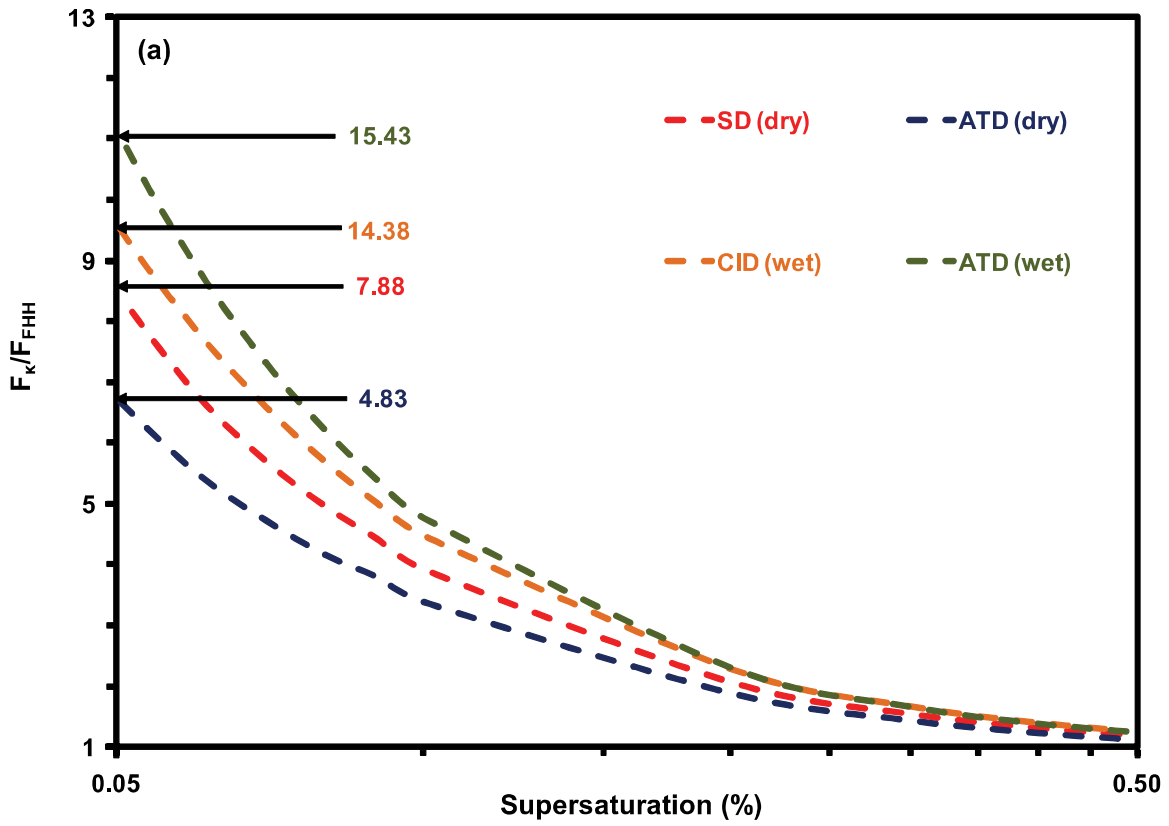


321
322

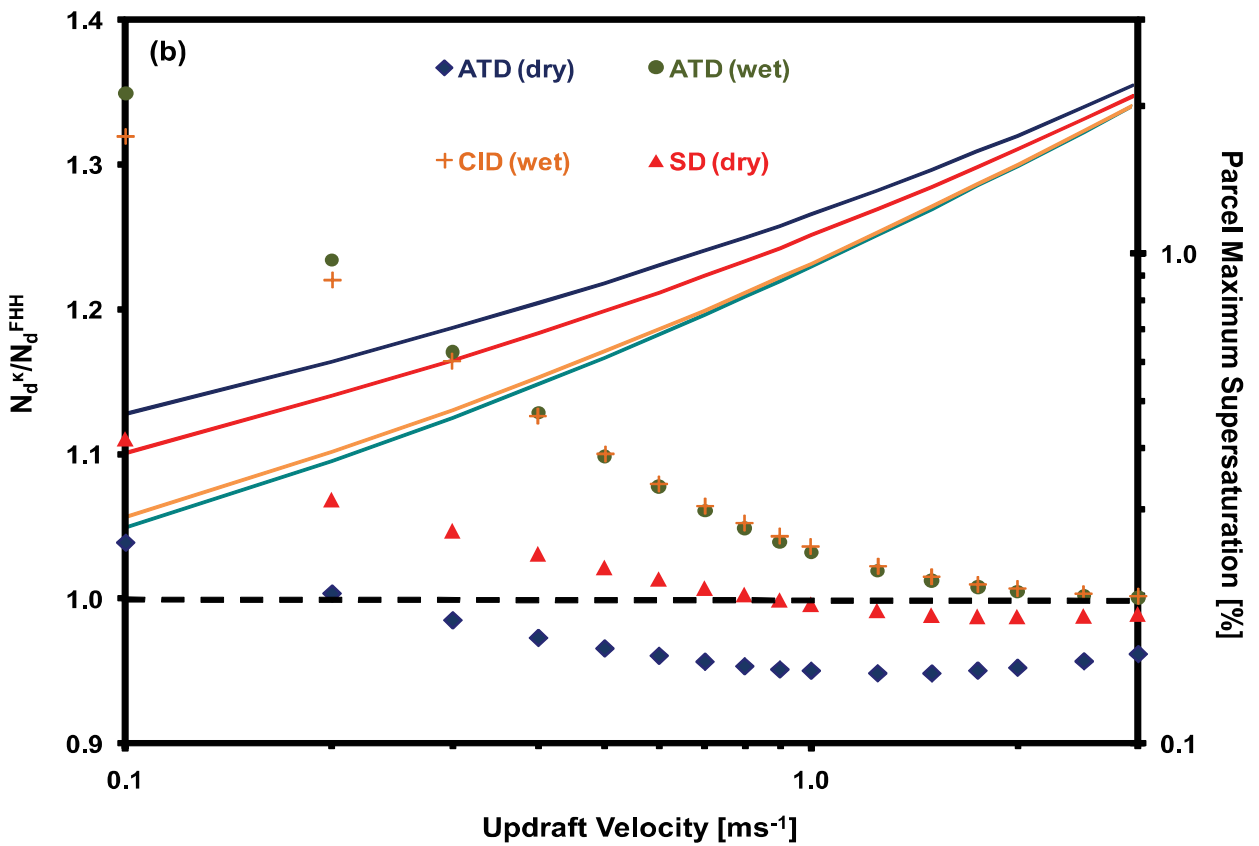


323
324

Figure 1



325
326



327
328

Figure 2